Phototunable Underwater Oil Adhesion of Micro/Nanoscale Hierarchical-Structured ZnO Mesh Films with Switchable Contact Mode

Dongliang Tian, Zhenyan Guo, Yiliang Wang, Wenxian Li, Xiaofang Zhang,* Jin Zhai,* and Lei Jiang*

Controllable surface adhesion of solid substrates has aroused great interest both in air and underwater in solving many challenging interfacial science problems such as robust antifouling, oil-repellent, and highly efficient oil/water separation materials. Recently, responsive surface adhesion, especially switchable adhesion, under external stimulus in air has been paid more and more attention in fundamental research and industrial applications. However, phototunable underwater oil adhesion is still a challenge. Here, an approach to realize phototunable underwater oil adhesion on aligned ZnO nanorod array-coated films is reported, via a special switchable contact mode between an unstable liquid/gas/solid tri-phase contact mode and stable liquid/liquid/solid tri-phase contact mode. The photo-induced wettability transition to water and air exists (or does not) in the micro/nanoscale hierarchical structure of the mesh films, playing important role in controlling the underwater oil adhesion behavior. This work is promising in the design of novel interfacial materials and functional devices for practical applications such as photo-induced underwater oil manipulation and release, with loss-free oil droplet transportation.

1. Introduction

Inspired from natural biological systems with special adhesion phenomena such as the lotus, geckos, rose petals, and fish, many studies have focused on preparing artificial surfaces with special functions.[1–4] Controllable surface adhesion of solid substrates, e.g., solid/solid contact adhesion, liquid/solid contact adhesion, has aroused great interest both in air and underwater in solving many challenging interface science problems such as robust antifouling, oil-repellent, and highly efficient oil/water separation materials.[5,6] As reported, chemical composition and geometrical structure are two main factors to govern surface adhesion.[7,8] Recently, responsive surface adhesion, especially switchable adhesion, under external stimulus such as light irradiation,[9] electric field,[10] magnetic field,[11] pH,[12] thermal treatment[13] and their combination (e.g., photoelectric cooperative fields),[14] in air has been paid more and more attention in fundamental research and industrial application. Besides, superoleophobic surfaces, in particular, underwater superoleophobic surfaces, have been widely investigated for their resistance to oil fouling and great potential in bio-adhesion, microfluidic technology, industrial metal cleaning, marine antifouling coating, et al.[4,15] Recently, photoresponsive materials' surface wettability switching between superhydrophilicity and superhydrophobicity with excellent intelligent controllability has been studied on the different solid substrate surfaces.[16] Based on the extreme wettability transition, the controllable water permeation and oil–water separation films have been developed, which have significant implications for the understanding and design of novel micro/nanofluidic devices.[17] Despite much progress in this field, phototunable underwater oil adhesion is still a challenge.

To achieve the photo-tunable underwater oil-adhesion, the underwater superoleophobic materials with different wetting state, i.e., contact mode, between UV illumination and storage in the dark are necessary. Micro/nanoscale hierarchical structured ZnO, e.g., aligned ZnO nanorod array-coated mesh film, is a good candidate for this purpose, because the hierarchical structured film can behave switching contact mode between UV illumination and storage in the dark.

Dr. D. Tian, Z. Guo, Prof. J. Zhai, Prof. L. Jiang
Key Laboratory of Bio-Inspired Smart Interfacial Science and Technology of Ministry of Education
School of Chemistry and Environment
Beihang University
Beijing, 100191, PR China
E-mail: tiandl@buaa.edu.cn; zhaijin@buaa.edu.cn
Prof. L. Jiang
Beijing National Laboratory for Molecular Sciences
Key Laboratory of Organic Solids
Institute of Chemistry
Chinese Academy of Sciences
Beijing, 100190, PR China
X. Zhang
Chinese Academy of Inspection and Quarantine
Beijing, 100123, PR China
E-mail: xfzhang_926@126.com
Dr. W. Li
Institute for Superconducting and Electronic Materials
University of Wollongong
NSW 2522, Australia
Y. Wang
China Information Security Certification Center
Beijing, 100020, PR China

DOI: 10.1002/adfm.201301799

Here we report an approach to realize phototunable underwater oil adhesion on the aligned ZnO nanorod array-coated film via special switchable contact mode between unstable liquid/gas/solid tri-phase contact mode and stable liquid/liquid/solid tri-phase contact mode. The photo-induced wettability transition to water and air existed or not in the micro/nanoscale hierarchical structure of the mesh films play important role in controlling the underwater oil adhesion behavior. This work is promising in the design of novel interfacial materials and functional devices for practical applications such as photo-induced underwater oil manipulation and release, and no loss oil droplet transportation.

2. Results and Discussion

2.1. Surface Wettability and Underwater Oil Adhesion Characteristics of the Fabricated Micro/Nanoscale Hierarchical-Structured ZnO Films

In this study, the aligned ZnO nanorod array is firstly prepared on the stainless steel mesh films to achieve the micro/nanoscale hierarchical structured ZnO films using a similar two-step solution approach reported in the literature.[17c] The aligned ZnO nanorod arrays are grown radically and exhibited uniformly along the entire length of every wire, with the average nanorod diameter of 68.3 ± 25.6 nm and the length of ~2 μm (see Figure S1 in the Supporting Information). As is reported in our former work,[17c] the surface wettability of the as-prepared micro/nanoscale hierarchical structured ZnO mesh films to water can switch between superhydrophobic after storage in the dark and superhydrophilic under UV irradiation. Compared with the surface wettability to water, the mesh film shows underwater superoleophobic to different type of oils both after storage in the dark and under UV irradiation, whereas the oil contact angles (OCAs) of the mesh film under UV irradiation are 1.7~7.2° bigger than those after storage in the dark owing to the superoleophilicity of the film in air (see Figure S2 in the Supporting Information).

In addition to surface wettability, the underwater oil adhesion force of the micro/nanoscale hierarchical structured ZnO mesh films is greatly affected by UV irradiation and storage in the dark. The underwater oil-adhesion force of the mesh film after storage in the dark and under UV irradiation was dynamically measured using our former established technique (**Figure 1**a).[4,5] In the underwater measurement process, an oil droplet (hexadecane, 5 μL) was contacted and squeezed with the mesh film surface then allowed to leave. The adhesion force between oil and surface was recorded by a highsensitivity microelectromechanical balance system. The mesh films behave special oil adhesion properties for different type of oils, such as 1,2-dichloroethane, hexadecane, vegetable oil, diesel oil and liquid paraffin, after storage in the dark and under UV irradiation. The oil adhesion force of the mesh film under UV irradiation are 19.0~32.6 μN smaller than those after storage in the dark (Figure 1b). The difference of the underwater OCAs and oil adhesion force of the mesh film between UV irradiation and storage in the dark is owing to the changing interfacial properies in water, i.e., the mesh film behaves superoleophilic in air after storage in the dark, while the mesh film behaves superoleophobic underwater under UV irradiation.

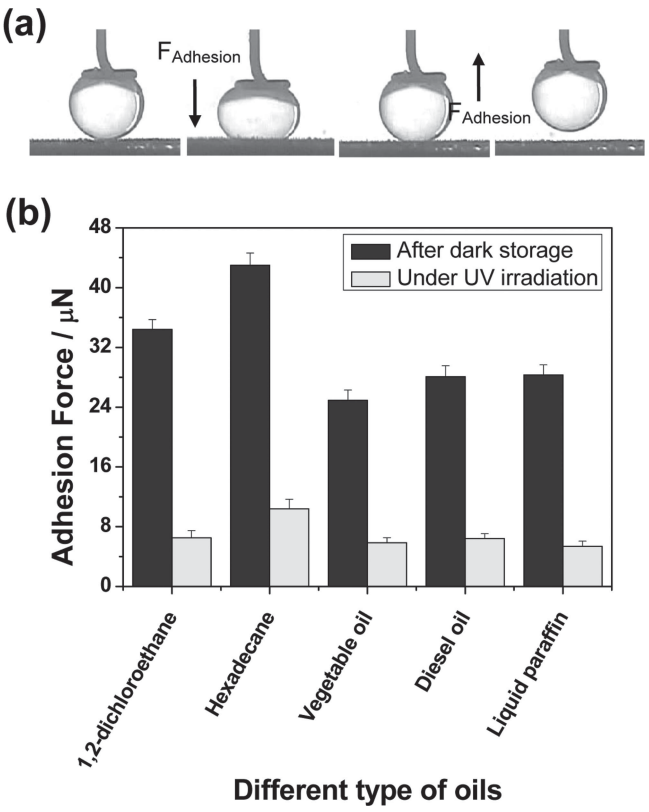

Figure 1. Underwater oil adhesion characteristics of the micro/nanoscale hierarchical structured ZnO mesh films. a) Underwater oil adhesion forces were measured on the micro/nanoscale hierarchical-structured ZnO mesh film after storage in the dark and under UV irradiation using oil droplets (Hexadecane, 5 μL) as detecting probes. Each measurement includes three steps: (left) before the oil droplet contacts the surface; (middle) the oil droplet is leaving the surface; (right) after the oil droplet leaves the surface. b) Oil adhesion characteristics of different oil droplets on the underwater mesh after storage in the dark and under UV irradiation.

2.2. Special Phototunable Underwater Oil Adhesion Characteristics of the Micro/Nanoscale Hierarchical-Structured ZnO Films

As mentioned above, both the wettability transition between superhydrophobicity and superhydrophilicity and underwater superoleophobicity with high and low oil adhesion force of the micro/nanoscale hierarchical structured ZnO films can be obtained by UV irradiation and storage in the dark. Thus the phototunable oil adhesion is feasible. To illustrate the phototunable underwater oil adhesion of the mesh films, the oil adhesion force–distance curves of the micro/nanoscale hierarchical-structured ZnO mesh films with the original pore size of ~120 μm were investigated. Taking the oil adhesion force of hexadecane oil for example, as shown in **Figure 2**, the force–distance curves, recorded before and after the underwater oil microdroplet contacted the micro/nanoscale hierarchical-structured ZnO mesh films surface, indicate that the oil adhesion force

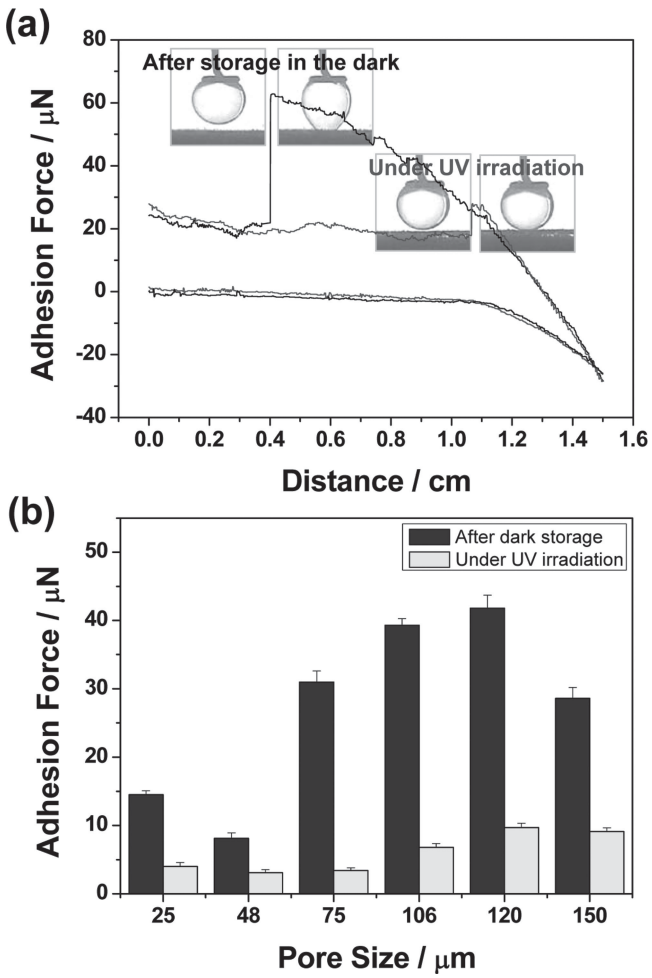

Figure 2. Special phototunable underwater oil adhesion characteristics of the micro/nanoscale hierarchical-structured ZnO mesh films. a) Force–distance curves recorded before and after the underwater oil microdroplet (hexadecane, 5 μL) contacted the as-prepared micro/nanoscale hierarchical-structured ZnO mesh film surface after storage in the dark and under UV irradiation. b) Underwater oil adhesion force of the micro/nanoscale hierarchical-structured ZnO mesh films under UV irradiation and after storage in the dark as a function of the pore size of the corresponding original stainless steel mesh films.

of the micro/nanoscale hierarchical-structured ZnO mesh film shows a high oil adhesion force of 43.2 ± 2.5 μN after storage in the dark and behaves a low oil adhesion force of 10.3 ± 2.1 μN under UV irradiation. (In the experiment, the light illumination part in the testing equipment is made of quartz glass). Moreover, the pore size of the corresponding mesh films has great influence on the oil adhesion force and the adhesion force difference between UV irradiation and storage in the dark. Further study shows that the underwater oil adhesion force of the micro/nanoscale hierarchical structured ZnO mesh films under UV irradiation and after storage in the dark changes as a function of the pore size of corresponding original stainless steel mesh films. The mesh film with the original pore size of ~120 μm behaves the highest adhesion force both UV irradiation and storage in the dark. Accordingly, these results indicated that the special interfacial properties of the micro/nanoscale hierarchical structured ZnO mesh film underwater and UV light illumination have important effect on the mesh films to achieve photo-responsive oil-adhesion characteristics.

2.3. Special Phototunable Underwater Air Bubble Adhesion Characteristics of the Micro/Nanoscale Hierarchical-Structured ZnO Films

To demonstrate the effects of the special interfacial properties of the micro/nanoscale hierarchical structured ZnO in water and external field on the photoresponsive oil-adhesion characteristics of the mesh films, following the air bubble-adhesion force of the micro/nanoscale hierarchical structured ZnO films was also investigated. As shown in **Figure 3**, the force–distance curves, recorded before and after the air bubble contacted the

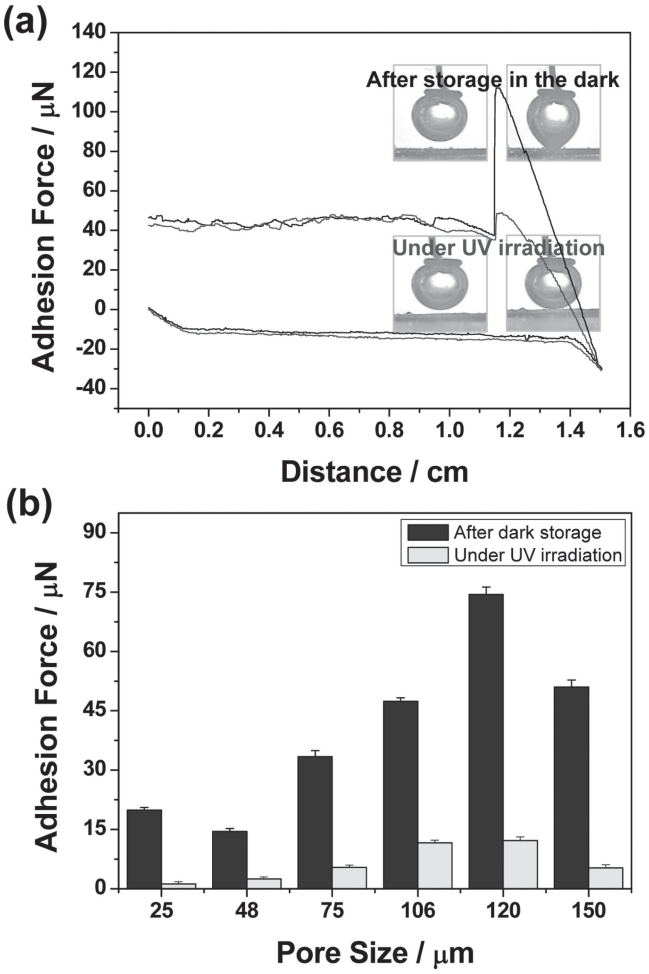

Figure 3. Special phototunable underwater air bubble adhesion characteristics of the micro/nanoscale hierarchical-structured ZnO mesh films. a) Force–distance curves recorded before and after the underwater air bubble (5 μL) contacted the as-prepared micro/nanoscale hierarchical-structured ZnO mesh film surface after storage in the dark and under UV irradiation. b) Underwater air bubble adhesion force of the micro/nanoscale hierarchical-structured ZnO mesh films under UV irradiation and after storage in the dark as a function of the pore size of the corresponding original stainless steel mesh films.

underwater micro/nanoscale hierarchical-structured ZnO mesh films surface, indicate that the air bubble adhesion force of the micro/nanoscale hierarchical-structured ZnO mesh film shows a high air bubble adhesion force of 75.4 ± 2.8 μN after storage in the dark and a low air bubble adhesion force of 13.6 ± 2.3 μN under UV irradiation. The further study shows that the underwater air bubble adhesion force of the micro/nanoscale hierarchical-structured ZnO mesh films under UV irradiation and after storage in the dark changes as a function of the pore size of the corresponding original stainless steel mesh films, which is consistent with the oil adhesion force mentioned above. The results indicate that the micro/nanoscale hierarchical-structured ZnO and UV light illumination also have important effects on the mesh films to achieve photoresponsive air bubble adhesion characteristics. Therefore, the special contact mode between the oil droplet/air bubble and the micro/nanoscale hierarchical-structured mesh film, i.e., air existed or not in the micro/nanoscale hierarchical structure, may be critical to cause the difference of oil/air bubble adhesion characteristics.

2.4. Mechanism of the Phototunable Underwater Oil/Air Bubble Adhesion Characteristics of the Micro/Nanoscale Hierarchical-Structured ZnO Films

To understand the phototunable oil adhesion mechanism of the micro/nanoscale hierarchical structured ZnO mesh films, the underwater contact mode between the oil droplet/air bubble and the micro/nanoscale hierarchical-structured mesh film were investigated after storage in the dark and under UV irradiation (**Figure 4**). In general, the micro/nanoscale hierarchical-structured mesh films are effective at preventing the liquid spontaneous transition from Cassie to Wenzel state due to the intrinsic advancing angle θ_a of the micro/nanoscale structure of mesh film,[18] which causes the intrusion pressure, ΔP, and determines its value, as described by the following Equation,[19]

$$\Delta P = \frac{2\gamma}{R} = -\, l\gamma(\cos\theta_a)/A \quad (1)$$

where γ is the interface tension, R is the radius of meniscus, l is the circumference of the mesh pore, A is the cross-sectional area of the pore, and θ_a is the advancing contact angle of oil on the surface in water.

From the Equation (1), for a certain kind of liquid on the micro/nanoscale hierarchical-structured ZnO mesh film with a certain square pore size, the advancing contact angle θ_a is the only variable and determines the ΔP value of the film. Thus the positive and negative values of ΔP can be judged by the advancing contact angle θ_a, and the exact value of the ΔP can also be obtained easily by the equation with all the exact values. In the experiment, we take the mesh film with the square pore size of 120 μm for example. According to the Equation 1, water (the interface tension γ values of water at 20 °C is 72.8 mN/m) can not immerge into the micro/nanoscale hierarchical structure of the superhydrophobic mesh film spontaneously and remain Cassie state in air after storage in the dark owing to $\Delta P > 0$ (water advancing contact angle $\theta_{a,w}$ of the ZnO mesh film after storage in the dark is ~155°). When the superhydrophobic mesh films are put into the water, small amount of air is trapped in the micro/nanostructures and formed air bubble on the micro/nanostructured mesh films (Figure 4a). While water will enter into the interspace of the nanorods of the mesh film completely under UV irradiation due to $\Delta P < 0$ (water advancing contact angle $\theta_{a,w}$ of the ZnO mesh film under UV irradiation is ~0°), and it is trapped in the micro/nanoscale hierarchical structures of the mesh film (Figure 4b). As a result, no air bubbles are formed on the micro/nanostructured mesh films under UV irradiation, and the contact mode changed from unstable liquid/gas/solid tri-phase contact mode to stable liquid/solid two-phase contact mode. Compared with water, hexadecane used as oil (the interface tension values of hexadecane at 20 °C is 27.2 mN/m) will immerge into the micro/nanoscale hierarchical structure of the film spontaneously in air even after storage in the dark owing to $\Delta P < 0$ (oil advancing contact angle $\theta_{a,o}$ of the ZnO mesh film after storage in the dark is ~0°),[17c] while oil can not completely enter into the micro/nanoscale structures of the mesh film spontaneously due to the air pressure and $\Delta P > 0$ (underwater oil advancing contact angle $\theta_{a,o}$ of the ZnO mesh film after storage in the dark is ~155°) of the mesh film to water (Figure 4c). Although a small portion of the oil invades into the micro/nanostructures of the mesh film, it may cause the mesh film to behave high oil adhesion force. When the mesh film is irradiated by UV light, the trapped water in the micro/nano-structures can improve the repellent force to oil, and oil can not invade into the micro/nanostructures of the mesh film spontaneously (Figure 4d) owing to the underwater static pressure of the mesh film to oil $\Delta P > 0$ (underwater oil advancing contact angle $\theta_{a,o}$ of the ZnO mesh film under UV irradiation is ~156°). Moreover, the trapped water in the micro/nanostructures can form the stable discontinuous liquid/liquid/solid triple-phase contact line and largely reduce or eliminate the oil adhesion force of the mesh film to oil. Clearly, the mesh film behaves different oil adhesion force with different contact mode when it is stored in the dark and irradiated under UV light.

To illustrate the existence of air in the micro/nanostructures of the mesh film underwater and further understand the effect of the trapped air on the phototunable oil adhesion force, the mechanism of the photo-tunable air bubble adhesion was also investigated. When air bubble touches the mesh film (after storage in the dark), it connects with the gas bubble stored in the micro/nanostructured mesh films to form one spontaneously in water, resulting in the high adhesion of the mesh film to air bubble (Figure 4e). Whereas a stable ball-like air bubble is formed on the mesh film when it touches the mesh film underwater under UV irradiation, because the stable discontinuous liquid/gas/solid triplephase contact line formed by the trapped water in the micro/nano-structures can largely improve the repellent force to air bubble, resulting in the low adhesion (Figure 4f). In addition, the micro/nanoscale hierarchical structured ZnO mesh film has important effect on the photoresponsive oil-adhesion characteristics. In general, as the mesh pore size increases, air/water trapped in the micro/nanostructured mesh films increases and the difference of oil adhesion between UV irradiation and storage in the dark is enhanced, however, when the pore size is large enough, air bubble can not be existed stably in the mesh films, as a result, the difference

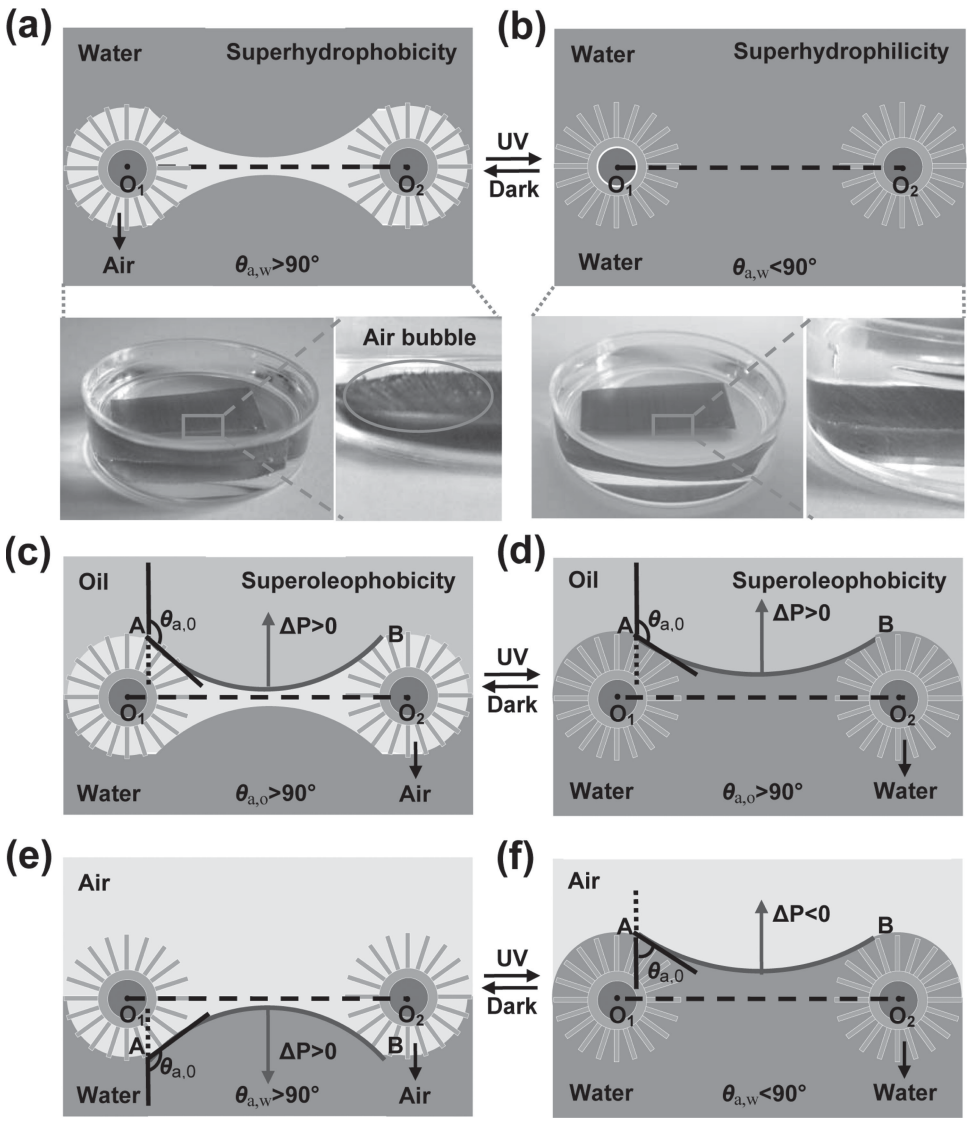

Figure 4. Schematic diagrams of the phototunable surface wettability and oil adhesion characteristics of the micro/nanoscale hierarchical-structured ZnO mesh films. a) When the superhydrophobic micro/nanoscale hierarchical-structured ZnO mesh films were put into the water, a small amount of air is trapped in the ZnO micro/nanostructures and forms air bubbles on the mesh films. b) When the superhydrophilic micro/nanoscale hierarchical-structured ZnO mesh films were put into the water, water completely wet and was trapped in the nanostructures of the mesh films and no air bubbles were formed on the mesh films. c) Oil cannot completely enter into the micro/nanoscale structures of the mesh film spontaneously due to the air pressure and $\Delta P > 0$ of the mesh film to water. d) Oil cannot invade into the micro/nanostructures of the mesh film spontaneously owing to the underwater static pressure of the mesh film to oil $\Delta P > 0$. e) When air bubble touches the mesh film in water, it connects with the gas bubble stored in the micro/nanostructured mesh films to form one bubble (after storage in the dark) spontaneously in water. f) When air bubble touches the mesh film, it forms stable ball on the mesh films (under UV irradiation) in water because the trapped water in the nanostructures can form the stable discontinuous tri-phase contact line and largely improve the repellent force to air bubble.

of oil adhesion between UV irradiation and storage in the dark is decreased again. These results strongly indicated whether air is trapped or not and the amount of the air in the micro/nanostructures determines the contact mode of oil on the ZnO mesh and also the adhesion force between oil and the ZnO mesh. Accordingly, the phototunable underwater air bubble/oil adhesion can be realized on the aligned ZnO nanorod array-coated mesh film with special switchable contact mode between unstable liquid/gas/solid tri-phase contact mode and stable liquid/liquid/solid tri-phase contact mode, and air existed or not in the micro/nanostructure of the mesh films are critical to achieve this.

3. Conclusions

This work has demonstrated an approach to realize phototunable underwater oil adhesion on the aligned ZnO nanorod array-coated film via special switchable contact mode between unstable liquid/gas/solid tri-phase contact mode and stable

liquid/liquid/solid tri-phase contact mode. The photo-induced wettability transition to water and air existed or not in the micro/nanoscale hierarchical structure of the mesh films play an important role in controlling the oil-adhesion behavior of underwater superoleophobic mesh films, and the phototunable underwater oil adhesion of the mesh films shows excellent controllability. This work is promising in the design of novel interfacial materials and functional devices for practical applications such as photo-induced underwater oil manipulation and release, and no loss oil droplet transportation.

4. Experimental Section

Preparation of the Aligned ZnO Nanorod Array-Coated Mesh Films: The preparation of the ZnO-coated mesh films used a similar procedure to that reported in the literature.[17c] In brief, the aligned ZnO nanorod array-coated mesh films were prepared via a two-step solution approach. First, ZnO sol was dip-coated onto the clean stainless steel mesh substrates and annealed at 420° to form the crystal seeds layer. Then the as-prepared substrates were suspended in an aqueous solution of zinc nitrate hydrate (0.025 M) and methenamine (0.025 M) at 85° for 15 h. Finally, they were removed from the solution, rinsed with deionized water, dried, and stored in the dark for two weeks before they were measured.

Wettability and Adhesion Force Switching of the Aligned ZnO Nanorod Array-Coated Mesh Films: All of the UV irradiation on every one of the ZnO-coated mesh films is ~0.5 h (a 500 W Hg lamp with a filter centered at 365 ± 10 nm) under the distance between UV light source and sample of ~15 cm to realize the superhydrophilicity and low adhesion of the film. After the UV irradiation, the ZnO-coated mesh films were placed in the dark for 7 days (or under atmosphere of O_2 for 2 days) to obtain a new superhydrophobicity and high adhesion of the films again for each sample. The wettability and adhesion force switching process can be repeated many times, and the time constants for adhesion force switching of the aligned ZnO nanorod array coated mesh films is consistent with the wettability switching of the same film in both directions, i.e., UV irradiation and storage in the dark. The switching adhesion force between UV irradiation and dark storage is promising in the design of the functional devices such as photo-induced underwater oil manipulation and release, and no loss oil droplet transportation.

Instruments and Characterization: The oil adhesion forces were measured using a high-sensitivity microelectromechanical balance system (Data-Physics DCAT 11, Germany) underwater. An 5 μL hexadecane droplet as oil droplet was suspended with a metal loop and controlled to contact with the surface to the aligned ZnO nanorod array coated mesh films at a constant speed of 0.005 mm s^{-1} and then to leave. The forces were recorded during the entire time. Hexadecane was taken as an example of detecting oils. The error bars in Figures 2 and 3 are calculated by the Standard Error of five measured results at the different positions of the same sample under the same condition. The adhesion experiments can be repeated accompany with the wettability switching between UV irradiation and storage in the dark.

Supporting Information

Supporting Information is available from the Wiley Online Library or from the author.

Acknowledgements

The authors are grateful for the financial support from the Chinese National Nature Science Foundation (21373001, 21003006, 21121001, 91127025, 51173190, 21234001), Beijing Natural Science Foundation (2133064), and the 973 Program (2013CB933004). The Chinese Academy of Sciences is gratefully acknowledged.

Received: May 25, 2013
Revised: September 1, 2013
Published online: October 27, 2013

[1] a) W. Barthlott, C. Neinhuis, *Planta* **1997**, *202*, 1; b) L. Feng, S. H. Li, Y. S. Li, H. J. Li, L. J. Zhang, J. Zhai, Y. L. Song, B. Q. Liu, L. Jiang, D. B. Zhu, *Adv. Mater.* **2002**, *14*, 1857; c) K. Koch, B. Bhushan, Y. C. Jung, W. Barthlott, *Soft Matter* **2009**, *5*, 1386; d) D. Quéré, *Rep. Prog. Phys.* **2005**, *68*, 2495; e) I. P. Parkin, R. G. Palgrave, *J. Mater. Chem.* **2005**, *15*, 1689.

[2] a) K. Autumn, Y. A. Liang, S. T. Hsieh, W. Zesch, W. P. Chan, T. W. Kenny, R. Fearing, R. J. Full, *Nature* **2000**, *405*, 681; b) H. Lee, B. P. Lee, P. B. Messersmith, *Nature* **2007**, *448*, 338; c) W. R. Hansen, K. Autumn, *Proc. Natl. Acad. Sci. USA* **2005**, *102*, 385; d) M. T. Northen, C. Greiner, E. Arzt, K. L. Turner, *Adv. Mater.* **2008**, *20*, 3905; e) M. H. Jin, X. J. Feng, L. Feng, T. L. Sun, J. Zhai, T. J. Li, L. Jiang, *Adv. Mater.* **2005**, *17*, 1977; f) F. M. Chang, S. J. Hong, Y. J. Sheng, H. K. Tsao, *Appl. Phys. Lett.* **2009**, *95*, 064102.

[3] L. Feng, Y. A. Zhang, J. M. Xi, Y. Zhu, N. Wang, F. Xia, L. Jiang, *Langmuir* **2008**, *24*, 4114.

[4] M. J. Liu, S. T. Wang, Z. X. Wei, Y. L. Song, L. Jiang, *Adv. Mater.* **2009**, *21*, 665.

[5] a) A. K. Geim, S. V. Dubonos, I. V. Grigorieva, K. S. Novoselov, A. A. Zhukov, S. Y. Shapoval, *Nat. Mater.* **2003**, *2*, 461; b) L. Ge, S. Sethi, L. Ci, P. M. Ajayan, A. Dhinojwala, *Proc. Natl. Acad. Sci. USA* **2007**, *104*, 10792; c) L. Qu, L. Dai, *Adv. Mater.* **2007**, *19*, 3844; d) R. Sheparovych, M. Motornov, S. Minko, *Adv. Mater.* **2009**, *21*, 1840; e) Y. Huang, M. Liu, J. Wang, J. Zhou, L. Wang, Y. Song, L. Jiang, *Adv. Funct. Mater.* **2011**, *21*, 4436.

[6] a) X. Zhang, L. Wang, E. Levanen, *RSC Adv.* **2013**, *3*, 12003; b) P. M. Mendes, *Chem. Soc. Rev.* **2008**, *37*, 2512; c) X. J. Liu, Y. M. Liang, F. Zhou, W. M. Liu, *Soft Matter* **2012**, *8*, 2070; d) Y. K. Lai, Z. Chen, C. J. Lin, *J. Nanoeng. Nanomanuf.* **2011**, *1*, 18; e) M. J. Vogel, P. H. Steen, *Proc. Natl. Acad. Sci. USA* **2010**, *107*, 3377; f) X. J. Liu, Q. A. Ye, B. Yu, Y. M. Liang, W. M. Liu, F. Zhou, *Langmuir* **2010**, *26*, 12377; g) E. V. Lebedeva, A. Fogden, *Environ. Sci. Technol.* **2010**, *44*, 9470; h) X. J. Huang, D. H. Kim, M. Im, J. H. Lee, J. B. Yoon, Y. K. Choi, *Small* **2009**, *5*, 90; i) R. La Spina, M. R. Tomlinson, L. Ruiz-Perez, A. Chiche, S. Langridge, M. Geoghegan, *Angew. Chem., Int. Ed.* **2007**, *46*, 6460; j) M. A. C. Stuart, W. T. S. Huck, J. Genzer, M. Muller, C. Ober, M. Stamm, G. B. Sukhorukov, I. Szleifer, V. V. Tsukruk, M. Urban, F. Winnik, S. Zauscher, I. Luzinov, S. Minko, *Nat. Mater.* **2010**, *9*, 101.

[7] a) R. Blossey, *Nat. Mater.* **2003**, *2*, 301; b) T. L. Sun, G. Y. Qing, B. L. Su, L. Jiang, *Chem. Soc. Rev.* **2011**, *40*, 2909; c) B. W. Xin, J. C. Hao, *Chem. Soc. Rev.* **2010**, *39*, 769; d) J. L. Zhang, Y. C. Han, *Chem. Soc. Rev.* **2010**, *39*, 676; e) X. J. Feng, L. Jiang, *Adv. Mater.* **2006**, *18*, 3063; f) X. Zhang, F. Shi, J. Niu, Y. G. Jiang, Z. Q. Wang, *J. Mater. Chem.* **2008**, *18*, 621; g) D. Quéré, *Annu, Rev. Mater. Res.* **2008**, *38*, 71; h) X. M. Li, D. Reinhoudt, M. Crego-Calama, *Chem. Soc. Rev.* **2007**, *36*, 1350; i) F. Xia, L. Jiang, *Adv. Mater.* **2008**, *20*, 2842; j) K. S. Liu, X. Yao, L. Jiang, *Chem. Soc. Rev.* **2010**, *39*, 3240; k) M. J. Liu, Y. M. Zheng, J. Zhai, L. Jiang, *Acc. Chem. Res.* **2010**, *43*, 368; l) M. J. Liu, L. Jiang, *Adv. Funct. Mater.* **2010**, *20*, 3753; m) X. Yao, Y. L. Song, L. Jiang, *Adv. Mater.* **2011**, *23*, 719; n) D. L. Tian, Y. L. Song, L. Jiang, *Chem. Soc. Rev.* **2013**, *42*, 5184.

[8] a) M. Callies, D. Quéré, *Soft Matter* **2005**, *1*, 55; b) H. Retsos, G. Gorodyska, A. Kiriy, M. Stamm, C. Creton, *Langmuir* **2005**, *21*, 7722; c) M. Kamperman, A. Synytska, *J. Mater. Chem.* **2012**, *22*,

19390; d) Z. Yoshimitsu, A. Nakajima, T. Watanabe, K. Hashimoto, *Langmuir* **2002**, *18*, 5818; e) Y. M. Zheng, X. F. Gao, L. Jiang, *Soft Matter* **2007**, *3*, 178; f) T. Verho, C. Bower, P. Andrew, S. Franssila, O. Ikkala, R. H. A. Ras, *Adv. Mater.* **2011**, *23*, 673; g) Y. K. Lai, X. F. Gao, H. F. Zhuang, J. Y. Huang, C. J. Lin, L. Jiang, *Adv. Mater.* **2009**, *21*, 3799; h) W. Lee, B. G. Park, D. H. Kim, D. J. Ahn, Y. Park, S. H. Lee, K. B. Lee, *Langmuir* **2010**, *26*, 8233; i) A. del Campo, C. Greiner, I. Alvarez, E. Arzt, *Adv. Mater.* **2007**, *19*, 1973; j) W. K. Cho, I. S. Choi, *Adv. Funct. Mater.* **2008**, *18*, 1089; k) A. Winkleman, G. Gotesman, A. Yoffe, R. Naaman, *Nano Lett.* **2008**, *8*, 1241; l) N. Zhao, Q. D. Xie, X. Kuang, S. Q. Wang, Y. F. Li, X. Y. Lu, S. X. Tan, J. Shen, X. L. Zhang, Y. Zhang, J. Xu, C. C. Han, *Adv. Funct. Mater.* **2007**, *17*, 2739; m) K. Uchida, N. Nishikawa, N. Izumi, S. Yamazoe, H. Mayama, Y. Kojima, S. Yokojima, S. Nakamura, K. Tsujii, M. Irie, *Angew. Chem. Int. Ed.* **2010**, *49*, 5942.

[9] a) C. Li, Y. Y. Zhang, J. Ju, F. T. Cheng, M. J. Liu, L. Jiang, Y. L. Yu, *Adv. Funct. Mater.* **2012**, *22*, 760; b) C. Li, F. T. Cheng, J. A. Lv, Y. Zhao, M. J. Liu, L. Jiang, Y. L. Yu, *Soft Matter* **2012**, *8*, 3730.

[10] a) T. N. Krupenkin, J. A. Taylor, T. M. Schneider, S. Yang, *Langmuir* **2004**, *20*, 3824; b) L. B. Zhu, J. W. Xu, Y. H. Xiu, Y.Y. Sun, D. W. Hess, C. P. Wong, *J. Phys. Chem. B* **2006**, *110*, 15945; c) X. D. Zhao, H. M. Fan, J. Luo, J. Ding, X. Y. Liu, B. S. Zou, Y. P. Feng, *Adv. Funct. Mater.* **2011**, *21*, 184; d) C. M. Ding, Y. Zhu, M. J. Liu, L. Feng, M. X. Wan, L. Jiang, *Soft Matter* **2012**, *8*, 9064; f) A. Pranzetti, S. Mieszkin, P. Iqbal, F. J. Rawson, M. E. Callow, J. A. Callow, P. Koelsch, J. A. Preece, P. M. Mendes, *Adv. Mater.* **2013**, *25*, 2181; g) C. C. A. Ng, A. Magenau, S. H. Ngalim, S. Ciampi, M. Chockalingham, J. B. Harper, K. Gaus, J. J. Gooding, *Angew. Chem. Int. Ed.* **2012**, *51*, 7706.

[11] a) X. Hong, X. F. Gao, L. Jiang, *J. Am. Chem. Soc.* **2007**, *129*, 1478; b) Z. J. Cheng, L. Feng, L. Jiang, *Adv. Funct. Mater.* **2008**, *18*, 3219.

[12] a) Q. F. Cheng, M. Z. Li, F. Yang, M. J. Liu, L. Li, S. T. Wang, L. Jiang, *Soft Matter* **2012**, *8*, 6740; b) X. Yu, Z. Q. Wang, Y. G. Jiang, F. Shi, X. Zhang, *Adv. Mater.* **2005**, *17*, 1289; c) L. D. Zarzar, P. Kim, J. Aizenberg, *Adv. Mater.* **2011**, *23*, 1442.

[13] a) S. Reddy, E. Arzt, A. del Campo, *Adv. Mater.* **2007**, *19*, 3833; b) L. Chen, M. Liu, H. Bai, P. Chen, F. Xia, D. Han, L. Jiang, *J. Am. Chem. Soc.* **2009**, *131*, 10467; c) E. Svetushkina, N. Puretskiy, L. Ionov, M. Stamm, A. Synytska, *Soft Matter* **2011**, *7*, 5691; d) C. Li, R. W. Guo, X. Jiang, S. X. Hu, L. Li, X. Y. Cao, H. Yang, Y. L. Song, Y. M. Ma, L. Jiang, *Adv. Mater.* **2009**, *21*, 4254; e) D. A. Wang, Y. Liu, X. J. Liu, F. Zhou, W. M. Liu, Q. J. Xue, *Chem. Commun.* **2009**, *45*, 7018; f) D. Wu, S. Z. Wu, Q. D. Chen, Y. L. Zhang, J. Yao, X. Yao, L. G. Niu, J. N. Wang, L. Jiang, H. B. Sun, *Adv. Mater.* **2011**, *23*, 545.

[14] a) D. L. Tian, Q. W. Chen, F.-Q. Nie, J. J. Xu, Y. L. Song, L. Jiang, *Adv. Mater.* **2009**, *21*, 3744; b) D. L. Tian, J. Zhai, Y. L. Song, L. Jiang, *Adv. Funct. Mater.* **2011**, *21*, 4519; c) X. Fan, X. Li, D. L. Tian, J. Zhai, L. Jiang, *J. Colloid Interface Sci.* **2012**, *366*, 1; d) Y. K. Lai, F. Pan, C. Xu, H. Fuchs, L. F. Chi, *Adv. Mater.* **2013**, *25*, 1682; e) Z. J. Cheng, H. Lai, M. Du, S. C. Zhu, N. Q. Zhang, K. N. Sun, *Soft Matter* **2012**, *8*, 9635.

[15] a) L. Lin, M. J. Liu, L. Chen, P. P. Chen, J. Ma, D. Han, L. Jiang, *Adv. Mater.* **2010**, *22*, 4826; b) M. Jin, J. Wang, X. Yao, M. Liao, Y. Zhao, L. Jiang, *Adv Mater* **2011**, *23*, 2861; c) Z. X. Xue, S. T. Wang, L. Lin, L. Chen, M. J. Liu, L. Feng, L. Jiang, *Adv. Mater.* **2011**, *23*, 4270.

[16] a) X. J. Feng, L. Feng, M. H. Jin, J. Zhai, L. Jiang, D. B. Zhu, *J. Am. Chem. Soc.* **2004**, *126*, 62; b) X. T. Zhang, O. Sato, A. Fujishima, *Langmuir* **2004**, *20*, 6065; c) H. Irie, T. S. Ping, T. Shibata, K. Hashimoto, *Electrochem. Solid-State Lett.* **2005**, *8*, D23; d) S. T. Wang, Y. L. Song, L. Jiang, *J. Photoch. Photobio C: Photochem. Rev.* **2007**, *8*, 18; e) R. Wang, K. Hashimoto, A. Fujishima, M. Chikuni, E. Kojima, A. Kitamura, M. Shimohigoshi, T. Watanabe, *Nature* **1997**, *388*, 431; f) H. S. Lim, J. T. Han, D. Kwak, M. H. Jin, K. Cho, *J. Am. Chem. Soc.* **2006**, *128*, 14458; g) C. L. Feng, Y. J. Zhang, J. Jin, Y. L. Song, L. Y. Xie, G. R. Qu, L. Jiang, D. B. Zhu, *Langmuir* **2001**, *17*, 4593; h) Z. Z. Zhang, J. Yang, X. H. Men, X. H. Xu, X. T. Zhu, *J. Adhes. Sci. Technol.* **2012**, *26*, 1083; i) X. H. Xu, Z. Z. Zhang, F. Guo, J. Yang, X. T. Zhu, *Appl. Surf. Sci.* **2011**, *257*, 7054; j) K. Y. Tan, J. E. Gautrot, W. T. S. Huck, *Soft Matter* **2011**, *7*, 7013.

[17] a) D. L. Tian, X. F. Zhang, J. Zhai, L. Jiang, *Langmuir* **2011**, *27*, 4265; b) D. L. Tian, X. F. Zhang, J. Zhai, L. Jiang, *Phys. Chem. Chem. Phys.* **2011**, *13*, 14606; c) D. L. Tian, X. F. Zhang, Y. Tian, Y. Wu, X. Wang, J. Zhai, Y. L. Song, L. Jiang, *J. Mater. Chem.* **2012**, *22*, 19652; d) L. B. Zhang, Z. H. Zhang, P. Wang, *NPG Asia Mater.* **2012**, *4*, 1; e) X. T. Zhu, Z. Z. Zhang, X. H. Xu, X. H. Men, J. Yang, X. Y. Zhou, Q. J. Xue, *Langmuir* **2011**, *27*, 14508; f) D. A. Wang, X. L. Wang, X. J. E. Liu, F. Zhou, *J. Phys. Chem. C* **2010**, *114*, 9938; g) X. Yao, J. Gao, Y. L. Song, L. Jiang, *Adv. Funct. Mater.* **2011**, *21*, 4270; h) W. Choi, A. Tuteja, S. Chhatre, J. M. Mabry, R. E. Cohen, G. H. McKinley, *Adv. Mater.* **2009**, *21*, 2190; i) L. P. Xu, J. Zhao, B. Su, X. L. Liu, J. T. Peng, Y. B. A. Liu, H. L. Liu, G. Yang, L. Jiang, Y. Q. Wen, X. J. Zhang, S. T. Wang, *Adv. Mater.* **2013**, *25*, 606.

[18] a) A. B. D. Cassie, S. Baxter, *Trans. Faraday Soc.* **1944**, *40*, 546; b) R. N. Wenzel, *Ind. Eng. Chem.* **1936**, *28*, 988.

[19] a) J. P. Youngblood, T. J. McCarthy, *Macromolecules* **1999**, *32*, 6800; b) A. Lafuma, D. Quéré, *Nat. Mater.* **2003**, *2*, 457.